Fast and Accurate ISAR focusing based on a Doppler Parameter Estimation Algorithm

Carlo Noviello, *Member, IEEE,* Gianfranco Fornaro, *Senior Member, IEEE,*
Paolo Braca, *Member, IEEE,* and Marco Martorella, *Senior Member, IEEE,*

***Abstract*—This work deals with Inverse Synthetic Aperture Radar (ISAR) autofocusing of non cooperative moving targets. The relative motion between the target and the sensor, which provides the angular diversity necessary for ISAR imagery, is also responsible for unwanted range migration and phase changes generating defocusing. In the case of non-cooperative targets, the relative motion is unknown: ISAR needs hence to implement an autofocus step (motion compensation) to achieve high resolution imaging. This task is typically carried out via the optimization of functionals based on general image quality parameters. In this work, we propose the use of a fast and accurate motion compensation algorithm based on the estimation of the Doppler parameters, thus fully coping with the nature of the imaging system. The effectiveness of the proposed method is proven on both simulated data and data acquired by operational systems.**

***Index Terms*—Inverse Synthetic Aperture Radar, Motion Compensation, Radar Imaging.**

I. Introduction

Inverse Synthetic Aperture Radar (ISAR) is a technology that exploits the sensor to the target motion to form a two-dimensional (2-D) detailed images of moving targets [1]. The transmission of large bandwidth pulses allows on one hand a high range resolution and a coherent combination of target echoes received at different aspect angles provides, on the other hand, a high cross-range resolution. The key element for high cross range resolution is the aspect angular diversity, which is either due to the target rotation or induced by the target cross range motion: in the latter, more realistic case, the unavoidable variation of the sensor to target distance leads also to the presence of phase terms that, if uncompensated at the focusing stage, may generate heavy defocusing. To achieve very high resolution imaging, such phase term has to be thus compensated by Motion Compensation (MoCo) procedures [1]. Typically, the target is not cooperative with the sensor: The required focusing parameters are therefore not known a-priori and must be estimated directly from the radar data via autofocusing implemented at the MoCo stage [1]. Several MoCo algorithms have been developed and proposed in the recent literature [1]–[9]: They are typically divided into parametric and non-parametric methods. Non-parametric techniques such as the so called envelope correlation method [2], the global range alignment [3], the Prominent Point Processing (PPP) [4] and the Phase Gradient Algorithm (PGA) [5] are very simple and popular, mainly because they do not require any model assumption. However, such methods can only achieve accuracies on the order of fractions of the range resolution whereas the required accuracy is on the wavelength fraction order. Other non-parametric methods, such as the Maximum Likelihood [6] technique and the Joint Time-Frequency Analysis (JTFA) [1] technique, have been also proposed. Such techniques typically divide the entire observation interval, referred to as coherent integration time (CIT) into multiple frames that are separately processed to generate multiple range-Doppler images. The relative motion in this case must be considered negligible within each frame to avoid target defocusing (blurring). The achieved cross range resolution is then lower than that obtainable with techniques exploiting the entire CIT. Advanced methods, such as the S-method [7] adopting a specific time frequency representation able to reduce the cross talk terms, can increase the CIT while limiting the blurring. Recently proposed parametric approaches, specifically the Image-Entropy [8] or Image Contrast-Based Technique (ICBT) [9], are recognized to be state of the art methods for achieving very high resolution ISAR images. A simple and computationally efficient ISAR autofocusing parametric approach, namely the Doppler Parameters Estimation Algorithm (DPEA) has been proposed in the context of refocusing of moving targets in SAR images [10]. DPEA is based on a very efficient Doppler parameters estimation module. SAR DPEA refocusing estimates the Doppler focusing parameters by updating the starting Doppler rate value estimated from orbital state vectors, see (31) in [10]. ISAR systems are typically fixed and for non cooperative targets there is no initial estimation of the radial acceleration. The method, as proposed in [10], is therefore not directly applicable to an ISAR system. In this work, we propose an improved version of DPEA able to perform an ISAR focusing, i.e. the focusing of moving targets sensed by a static radar. In this work we address the development of an approach able to operate regardless of the a-priori knowledge of the initial estimates of the Doppler parameters. With respect to known parametric approaches based on optimization of general image quality measurements, i.e. ICBT or entropy minimization, the proposed approach exploits the intrinsic characteristics of the acquired radar signal, thus fully coping with the specific (Doppler) peculiarities of the radar imaging system. Thanks to this feature, as shown in the experimental results section, DPEA generally allows for focusing capabilities comparable or

C. Noviello and G. Fornaro are with the Institute for Electromagnetic Sensing of the Environment (IREA-CNR), Naples, 80124, Italy e-mail: noviello.c@irea.cnr.it, fornaro.g@irea.cnr.it.

P. Braca is with Maritime Research and Experimentation (CMRE-NATO), Viale San Bartolomeo, 400, La Spezia, Italy, paolo.braca@cmre.nato.int

M. Martorella is with Department of Ingegneria dell'Informazione, University of Pisa, Pisa, 56122, Italy, e-mail: m.martorella@iet.unipi.it.

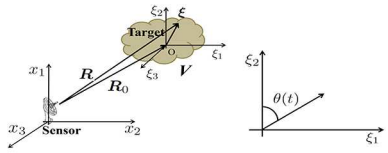

Fig. 1: Reference geometry of the ISAR system.

even better than classical parametric based methods, but, to be achieved with reduced computational costs. The latter feature is particularly appealing for operational purposes especially for quasi real time imaging of moving targets for harbour traffic monitoring.

II. Signal Model

To describe the received signal, we refer to the geometry depicted in Figure 1 where the sensor is located at $(0,0,h)$ in the system of coordinates (x_1,x_2,x_3) and we consider also the reference system (ξ_1,ξ_2,ξ_3) on the target: the latter is assumed to move along an arbitrary trajectory. In a typical ISAR scenario, by assuming that the target size is significantly smaller than the radar-target distance (iso-range approximation): $R(\boldsymbol{\xi},t_s) \simeq R_0(t_s)+\xi_1 sin(\theta(t_s))+\xi_2 cos(\theta(t_s))$, where $R(\boldsymbol{\xi},t_s)$ is the distance at time t_s between the sensor and a scatterer, $R_0(t_s)$ is the modulus of the vector $\boldsymbol{R}_0(t_s)$ which locates the position of the reference point on the target (see Figure 1). We suppose that the sensor transmits an ideal pulse with the bandwidth B at a carrier frequency f_0 over a CIT of T [1]. In the following we will always assume the frequency f and the slow-time t_s be limited in $|f-f_0| \leqslant B/2$ and $|t_s| \leqslant T/2$. The signal backscattered from the target to the sensor, as function of the frequency f and the slow-time t_s is given by:

$$S_b(f,t_s) = e^{-j4\pi\frac{f}{c}R_0(t_s)} \int\int \gamma(\xi_1,\xi_2) \\ e^{-j4\pi\frac{f}{c}(\xi_1 sin(\theta(t_s))+\xi_2 cos(\theta(t_s)))} d\xi_1 d\xi_2. \quad (1)$$

where c is the speed of light; (ξ_1,ξ_2) are the cross-range and (slant) range coordinates respectively defining the target imaging plane and $\gamma(\xi_1,\xi_2)$ is the reflectivity function representing the projection of the 3-D reflectivity function on the image plane [1]. Equation (1) is the classical expression of the ISAR signal: It highlights that the received signal can be considered as a the Fourier Transformation (FT) of the backscattering function associated with the target in a polar domain. Generally, the CIT T is small and the rotation may be assumed uniform so that: $\theta(t_s) \simeq \Omega_{eff} t_s$ where Ω_{eff} is the modulus of the effective rotation vector $\boldsymbol{\Omega}_{eff}$. The received signal in (1) can be thus rewritten as:

$$S_b(f,t_s) \approx e^{-j4\pi\frac{f}{c}R_0(t_s)}\Gamma(f,t_s) \quad (2)$$

where letting, $R_{x_1} = c/(2f_0\Omega_{eff}T)$ (cross-range resolution), we have:

$$\Gamma(f,t_s) = \int\int \gamma(\xi_1,\xi_2) e^{-j2\pi\left(R_{x_1}T\right)\xi_1 t_s} e^{-j2\pi\frac{2f}{c}\xi_2} d\xi_1 d\xi_2. \quad (3)$$

In coherent imaging contexts the reflectivity is assumed to have a (real) positive, i.e., zero phase, autocorrelation [11]. Hence, hereafter we assume that the autocorrelation of Γ, i.e. R_Γ is (real) and positive, so that the FT of R_Γ, i.e., $|\gamma|^2$ may be assumed concentrated around the origin. To reconstruct the ISAR image, however, a key step is represented by the MoCo stage, which consists of evaluating and compensating the phase term $exp\{-j(4\pi f/c)R_0(t_s)\}$. Following this operation a simple inverse FT provides the wanted target reconstruction: This approach is known as Range-Doppler approach [1]. The Point Spread Function (PSF), i.e. the impulse Response Function ($\gamma(\xi_1,\xi_2) = \gamma_0\delta(\xi_1,\xi_2)$) can be easily derived as being equal to:

$$s_I(\tau,f_d) = \gamma_0 TB|sinc[B(\tau-\frac{2\xi_2}{c})]||sinc[T(f_d-\frac{\xi_1}{R_{x_1}T})]|, \quad (4)$$

where $sinc(x) = sin(\pi x)/(\pi x)$, τ is the round trip delay, f_d is the doppler frequency.

III. Doppler Parameters Estimation Algorithm

MoCo procedure is a fundamental step for the generation of high resolution ISAR images. In the case of non cooperative targets, the motion parameters are unknown to the sensor. To achieve high cross range resolution, the term $R_0(t_s)$ has to be estimated directly from the data and removed. DPEA exploits the Doppler properties of the ISAR signal to estimate the target motion parameters for MoCo. We assume that the relative motion between the sensor and the target is smooth and regular so that the distance $R_0(t_s)$ can be well approximated by second order Taylor polynomial:

$$R_0(t_s) \approx R_0 + v_R t_s + a_R t_s^2, \quad (5)$$

where $v_R = \dot{R}_0(0)$ and $a_R = \ddot{R}_0(0)/2$: dots and double dots represent the first and second derivatives with respect to the time. The coefficients v_R and a_R are the radial component of the target velocity and acceleration, respectively: They are also related to the frequency Doppler parameters (the Doppler centroid f_{DC} and the Doppler rate f_{DR}) as follows:

$$f_{DC} = \frac{2f}{c}v_R \qquad f_{DR} = \frac{4f}{c}a_R. \quad (6)$$

Both motion coefficients v_r and a_r, can be thus retrieved by estimating the Doppler centroid and the Doppler rate parameters. We refer to (2) and hereafter, just for sake of simplicity, we reason with a one dimensional signal by neglecting the dependence on the frequency, thus by letting $f = f_0$. We have therefore:

$$S_{b_0}(f,t_s) \triangleq e^{-j2\pi(f_{DC}t_s+\frac{f_{DR}}{2}t_s^2)}\Gamma_0(t_s), \quad (7)$$

where, for the sake of simplicity, we have substituted the relationship between the motion parameters and the Doppler parameters as explained in the formula (6) and $\Gamma_0(t_s) = \Gamma(f=f_0,t_s)$.

A. Doppler Centroid Estimation

The Doppler centroid is a key parameter for cross-range focusing: It represents the average Doppler shift which affects the backscattered signal. The Doppler centroid estimation is obtained by re-adapting the algorithm proposed in [12] in the

context of classical SAR focusing. With reference to (7), let us define the following function:

$$S_0(t_s) \triangleq e^{-j\pi f_{DR} t_s^2} \Gamma_0(t_s). \tag{8}$$

Therefore, the signal defined in formula (7) can be easily written as:

$$S_{b_0}(t_s) = S_0(t_s) e^{-j2\pi f_{DC} t_s} \tag{9}$$

The (discrete time) autocorrelation function $R_s(k)$ is therefore:

$$R_{S_{b_0}}(k) = R_{S_0}(k) e^{-j2\pi k T_R f_{DC}}. \tag{10}$$

with R_{s_0} being the autocorrelation function of the sampled version ($t_s = kT_R \quad k = 0, 1, \ldots, N-1$) of the signal $S_0(t_s)$. As already mentioned in Section II we assume that R_Γ is real and positive. This assumption stems from the fact that the Fourier spectrum of the received signal along the slow time is peaked around the doppler frequency associated with the radial velocity of the target. According to this consideration, by measuring the phase of the correlation function defined in (10), it is possible to estimate the Doppler centroid as follows:

$$\hat{f}_{DC}(k) = \frac{1}{2\pi k T_R} arg\{R_{S_{b_0}}(k)\}, \tag{11}$$

where arg is the phase extraction operator. A Maximum Likelihood estimation of f_{DC} can be achieved as in [13]. A robust and accurate centroid estimation, close to the Maximum Likelihood estimation derivable when the observed scene is described by a withe Gaussian process can be achieved by setting $k = 1$ in (11).

B. Doppler Rate Estimation

The algorithm for the estimation of the Doppler rate takes inspiration from a previous algorithm developed for focusing SAR images acquired by satellite sensors [14]. It exploits the following linear mapping: $f_d = f_{DR} t_s$ between the Doppler frequency f_d and the slow-time t_s. The rationale of the method is that for $f_{DR} \neq 0$ two sub looks corresponding to different doppler windows provide, according to linear mapping: $f_d = f_{DR} t_s$, images centered at different t_s. To estimate the slope of this linear mapping, the proposed algorithm exploits the cross correlation between images generated by at least two sub-apertures. We assume that the Doppler centroid term has been compensated as explained in the previous sub-section, and, therefore we next refer to the signal $S_0(t_s)$ defined in formula (8). It can be shown that the cross correlation function between two sub-looks, S_1 and S_2 can be written as:

$$R_{s_1 s_2}(\nu) = FT\{R_{\Gamma_0}(\eta) R_{\Gamma_0}(-\eta) e^{-j2\pi f_{DR} \frac{T}{2} \eta} \Lambda^2(\tfrac{\eta}{T})\} = A\left[\tfrac{(\nu - f_{DR} T/2)}{T}\right]. \tag{12}$$

where $\Lambda()$ is the classical triangular function. A thorough mathematical derivation of the above formula is provided in the supplementary file [15]. From (12), it is seen that A is defined as the FT of $\{R_{\Gamma_0}(\eta) R_{\Gamma_0}(-\eta) \Lambda^2(\frac{\eta}{T})\}$: the latter is a real, even and positive function. Therefore, reasoning as in the previous subsection, it can be concluded that A achieves its maximum value in the origin. In the simplified case of a single scatterer $R_{\Gamma_0}(\eta)$ is a constant function and therefore A reduces to the convolution between two squared $sinc()$ functions. In any case, i.e. either in the presence of a dominant scatterer on in a more general situation of a target with distributed scatterers, the cross-correlation between the two sub-looks produces a maxima at the position $f_{DR} T/2$. Accordingly, by measuring the maximum of the cross-correlation function, that is:

$$\widehat{\nu}_{max} = \arg\max_{\nu} \{R_{s_1, s_2}(\nu)\} = f_{DR} \frac{T}{2} \tag{13}$$

it is possible to achieve the estimation of the Doppler rate as: $\widehat{f}_{DR} = \widehat{\nu}_{max} \frac{2}{T}$.

C. Overall Processing Procedure

In this section we provide an overall description of the ISAR imaging based on the DPEA for MoCo. The block diagram of the proposed procedure is shown in Figure 2. We start

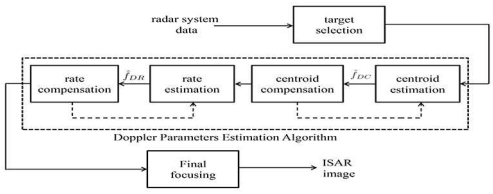

Fig. 2: Block diagram of DPEA processor. The dashed arrows represent the possibility to iterate the estimation procedures.

from data generated by a generic radar system, it could be a classical pulsed radar or Frequency Modulate Continuous Wave (FMCW) radar. The target selection module in Figure 2, also known as cropping, is necessary for extraction of the data relative to the target of interest, which is typically present together with clutter and other targets. After the cropping of the data, as illustrated in Figure 2, the DPEA first of all estimates the Doppler centroid by exploiting the procedure described in the Section III-A and then operates its compensation. It is worth noting that this compensation is carried out in the range frequency domain in order to also accommodate the so called range walk (linear component of the target range migration). In order to improve the estimation, the process can be iterated (see the dashed line) until the difference between the two iterations is below a pre-set threshold: convergence typically requires very few iterations. The algorithm performs subsequently the Doppler rate estimation by exploiting the procedure described in the Section III-B. The estimated value is used to compensate, again in the range frequency domain, the whole range migration. Similarly to the centroid compensation, the rate estimation and compensation steps are iterated. Iterations are typically very limited. Finally, the algorithm performs the "Final focusing" block for generating the Range-Doppler ISAR image with the estimated parameters.

IV. Experimental Results

This section aims at demonstrating the effectiveness of the proposed technique with tests on both simulated data and data acquired by operational systems: All sensors, including the simulated one, operate at X-Band (with a carrier frequency of 9.6GHz) with 0.5m of slant range resolution (the transmitted

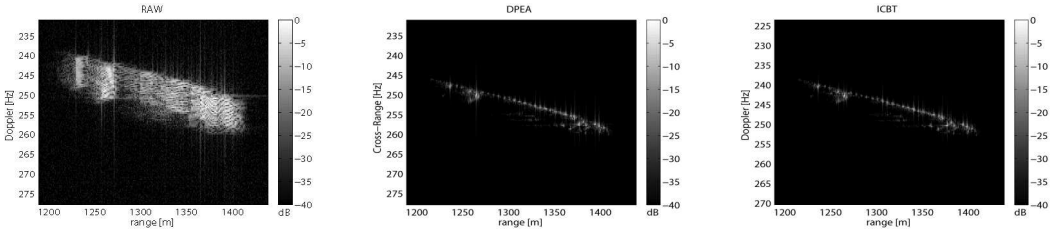

(a) Unfocused (b) Focused by DPEA. (c) Focused by ICBT.

Fig. 4: First case study with data acquired by the CMRE operational system: comparison between DPEA and ICBT.

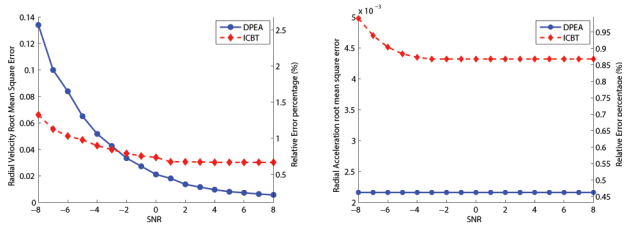

(a) RMSE velocity. (b) RMSE acceleration.

Fig. 3: Root Mean Square error comparison analysis between DPEA and ICBT in the case of AWGN.

bandwidth is 300 MHz). Results achieved by the proposed technique have then been compared with those obtained by a state of art MoCo parametric technique for accurate and fast ISAR imaging, namely: the Image-Contrast Based Technique (ICBT) autofocusing algorithm [9].

A. Simulated Data

The first test is carried out on a simulated data-set. A point target simulator has been developed, and, data corresponding to a ship target supposed to be moving with a rectilinear trajectory with uniformly accelerated motion with a constant radial velocity of 5m/s and a radial acceleration of 0.5m/s have been generated. The CIT is $1s$ and the Pulse Repetition Frequency (PRF) is 650Hz. The simulations have been exploited for comparing the estimation performances of the DPEA and ICBT methods in the presence of noise; to this end the data has been corrupted by additive white Gaussian noise. Monte Carlo simulations have been run to quantify the estimation performances for each motion component: a total of 500 trials have been processed for each SNR value with the aforementioned simulated ISAR system. From the statistical analysis shown in Figure 3, it is seen that the proposed DPEA method performs with better accuracy than the ICBT method both in the radial velocity and radial acceleration. This is related to the fact that the DPEA is based on the measurement and optimization of quantities related to the Doppler phase history which is a key feature in the imaging mechanism. With reference to the radial velocity, ICBT performs better for very low SNR: This is probably due to the high contrast characteristics of the simulated scene. The flatness of the DPEA curve indicates a very high robustness of the proposed Doppler rate estimation procedure to achieve high accuracy levels. Finally, as for the computational costs, it should be pointed out that the application of optimization procedure generally carried out in ICBT was not possible because of the presence of local maxima in the image contrast function corresponding to cases of low SNR. Accordingly, the ICBT was run with an exhaustive brute force search which is extremely time consuming.

B. Data acquired by operational systems

In order to validate and test the proposed technique in different operative conditions and in the presence of different clutter scenarios, the DPEA has been tested with two independent X-band radar systems. The results obtained by using DPEA have been again compared with those generated by ICBT. The comparison analysis between the two different algorithms has been carried out by considering the following features: image visual quality, image contrast, entropy of the image intensity, peak value of the image intensity and computational load.

1) First Case Study: In the first case study, the DPEA has been tested with a maritime X-band radar system data-set owned by Centre for Maritime Research & Experimentation (CMRE) in the Gulf of La Spezia (Italy). The CIT is in this case 3.349s and the PRF is $611,546$Hz typical operative range values are between 1 and 5 Km. We have considered the problem of focusing the moving ship showed in Figure 4(a). As is evident from Figure 4(a) the target image is affected by considerable de-focusing, in fact, the range-Doppler target image shows a significant blurring and thus it is not possible to identify the shape of the vessel. The images obtained by using the DPEA and ICBT autofocusing techniques are shown in Figures 4(b) and 4(c): dB scales with respect to the maximum values have been adopted; the horizontal axis corresponds to the (slant) range from the first pixel before cropping, the vertical axis to the Doppler. The scaling from Doppler to cross-range requires the estimation of the magnitude of the effective rotation vector [1]. From the visual point of view, both algorithms have achieved satisfactory image focusing: the contours of the ship are much more delineated than in the original image. The results in terms of image contrast, entropy and peak reflect the visual inspection results. Such results are shown in Table I. As shown in Table I, ICBT achieves a slight higher contrast but a higher value of entropy and a lower peak value. DPEA is however more than three times faster than ICBT.

2) Second Case Study: The testing data-set is relative to a test of a system carried out within the experiments of the NATO SET-196 Task Group on “Multichannel/Multistatic

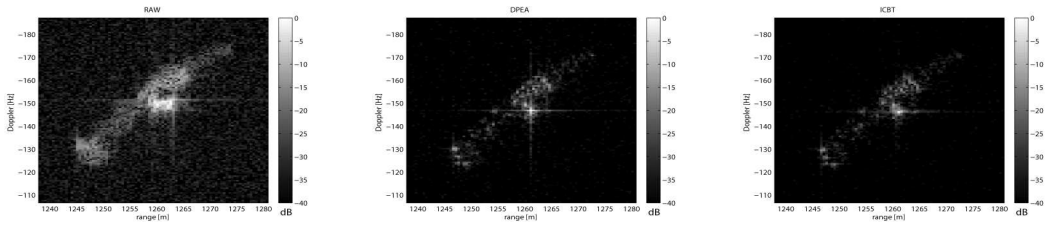

(a) Unfocused (b) Focused by DPEA. (c) Focused by ICBT.

Fig. 5: Second case study with data acquired by the HABITAT operational system: comparison between DPEA and ICBT.

TABLE I: Comparison Parameters for first case study

Parameters	***Raw Data***	***DPEA***	***ICBT***
Contrast	2.563	3.963	3.959
Entropy	8.806	6.082	6.056
Peak	5.310×10^6	3.486×10^7	3.775×10^7
Computational load, s		0.528	1.756

TABLE II: Comparison Parameters for second case study

Parameters	***Raw Data***	***DPEA***	***ICBT***
Contrast	1.484	1.589	1,591
Entropy	7.400	6.475	6.333
Peak	3.218×10^6	8.718×10^6	1.007×10^7
Computational load		0.253 s	0,647 s

Radar Imaging of Non-Cooperative Targets" in Livorno (Italy) in 2014 by using the HABITAT radar system. The Figure 5(a) shows the cropping of a moving ship, in the range-Doppler. The CIT is in this case of 1.5s and the PRF is again $611,546$Hz. As can be seen, the range-Doppler image of the target, also in this case, is affected by a rather large defocusing involving blurring effects: The different point scatterers representative of the ship are not easily distinguishable. Figures 5(b) and 5(c) show the Range-Doppler images of target refocused with the DPEA and the ICBT techniques, respectively. From a visual inspection, both methods achieve satisfactory results. In fact, also in this case the contours of the ship are much more delineated than in the original image and the point spread function of a dominant scatterer is well concentrated. What was previously stated by the visual inspection, is also confirmed by evaluating the quality imaging parameters described in Table II. The DPEA achieves, albeit very slightly, a higher entropy, a lower contrast and a lower peak. However, the visual inspection of the images in 5(c) appears to be in favor of the DPEA: The contours of the ship in Figure 5(b) look more delineated than in the ICBT result, i.e. Figure 5(c). The computational load analysis again confirms the advantages of DPEA whose processing time is more than halved with respect to ICBT.

V. Conclusion

This work has described a simple, fast and accurate ISAR focusing algorithm that exploits the Doppler characteristics of the radar signal. The effectiveness of the proposed algorithm has been proven by testing it on simulated data and on two different data-sets acquired by operative radar systems. It has been shown that it is a valid alternative to classical methods being able to achieve, with the same final image quality, robustness and a computational time gain.

ACKNOWLEDGMENT

The authors thank the NATO SET-196 Research Task Group and the Centre for Maritime Research & Experimentation for providing the data acquired by operative radar systems. This work has been partially funded by MIUR under the project PON "HArBour traffIc OpTimizAtion SysTem" (HABITAT).

References

[1] V. C. Chen and M. Martorella, *Inverse Synthetic Aperture Radar Imaging Principles, Algorithms and Applications*, Shitech Pub., 2014, vol. 1.
[2] C. C. Chen and H. C. Andrews, "Target-Motion-Induced Radar Imaging," *IEEE Trans. Aerosp. Electron. Syst.*, no. 1, pp. 2–14, Jan. 1980.
[3] J. Wang and D. Kasilingam, "Global Range Alignment for ISAR," *IEEE Trans. Aerosp. Electron. Syst.*, vol. 39, no. 1, pp. 351–357, Mar. 2003.
[4] G. Delisle and H. Wu, "Moving Target Imaging and Trajectory Computation using ISAR," *IEEE Trans. Aerosp. Electron. Syst.*, vol. 30, no. 3, pp. 887–899, Jul. 1994.
[5] D. Wahl, P. Eichel, D. Ghiglia, and C. Jakowatz Jr, "Phase Gradient Autofocus a Robust Tool for High Resolution SAR Phase Correction," *IEEE Trans. Aerosp. Electron. Syst.*, vol. 30, no. 3, pp. 827–835, Jul. 1994.
[6] F. Berizzi and G. Pinelli, "Maximum-likelihood ISAR Image Autofocusing Technique Based on Instantaneous Frequency Estimation," *IEE Proc. Radar Sonar Navig.*, vol. 144, no. 5, pp. 284–292, Oct. 1997.
[7] T. Thayaparan, L. Stankovic, C. Wernik, and M. Dakovic, "Real-Time Motion Compensation, Image Formation and Image Enhancement of Moving Targets in ISAR and SAR using S-Method Based Approach," *IET Signal Processing*, vol. 2, no. 3, pp. 247–264, Sept. 2008.
[8] L. Xi, L. Guosui, and J. Ni, "Autofocusing of ISAR Images Based on Entropy Minimization," *IEEE Trans. Aerosp. Electron. Syst.*, vol. 35, no. 4, pp. 1240–1252, Oct. 1999.
[9] M. Martorella, F. Berizzi, and B. Haywood, "Contrast Maximization Based Technique for 2-D ISAR Autofocusing," *IEE Proc. Radar Sonar Navig.*, vol. 152, no. 4, pp. 253–262, Aug. 2005.
[10] C. Noviello, G. Fornaro, and M. Martorella, "Focused SAR Image Formation of Moving Targets Based on Doppler Parameter Estimation," *IEEE Trans. Geosci. Remote Sens.*, vol. 53, no. 6, pp. 3460–3470, Jun. 2015.
[11] L. I. Goldfischer, "Autocorrelation Function and Power Spectral Density of Laser-Produced Speckle Patterns," *Journal of Optical Society of America*, vol. 55, no. 3, pp. 247–253, Mar. 1965.
[12] S. N. Madsen, "Estimating the Doppler Centroid of SAR Data," *IEEE Trans. Aerosp. Electron. Syst.*, vol. 25, no. 2, pp. 134–140, Mar. 1989.
[13] R. Bamler, "Doppler Frequency Estimation and the Cramer-Rao bound," *IEEE Trans. Geosci. Remote Sens.*, vol. 29, no. 3, pp. 385–390, May 1991.
[14] J. C. Curlander and R. N. McDonough, *Synthetic Aperture Radar: System and Signal Processing*, Wiley, New York, 1991.
[15] C. Noviello, G. Fornaro, P. Braca, and M. Martorella, "Fast and Accurate ISAR focusing based on a Doppler Parameter Estimation Algorithm: Supplementary Material," to be made available online: https://zenodo.org.